

## SOOT FORMATION RATES IN TWO LAMINAR ETHYLENE DIFFUSION FLAMES

D.R. HONNERY, S. DJINGGA and J.H. KENT

Department of Mechanical Engineering  
University of Sydney, NSW 2006  
AUSTRALIA

### ABSTRACT

A soot reaction rate model based on temperature and mixture fraction is examined to determine whether it can be used in flames with different residence times. Soot formation rates are deduced from soot concentration measurements made in two laminar ethylene diffusion flames. These are correlated with predicted local mixture fractions and measured temperatures. Significant differences in the correlations are found for the two flames. The results indicate that additional considerations are required to model soot formation rates in diffusion flames and point to mixing rates as having an important influence.

### INTRODUCTION

The presence of soot in practical diffusion flames such as in gas turbine combustors, diesel engines and furnaces has long been of interest. Soot is important when modelling combustion because it is a pollutant and because soot particles radiate heat strongly. The chemical mechanism for soot formation is not established. Some proposals for the simpler situation of premixed flame soot formation (Frenklach and Warnatz (1987)) are lengthy and high in computer requirements. There is therefore a need to determine whether relatively simple soot formation models can be established in terms of available parameters in diffusion flames.

The approach here is to use local temperature and mixture fraction in the diffusion flame field as the parameters with which to correlate local soot formation rates. Mixture fraction is a measure of local stoichiometry. It is the mass fraction of elements originating in the fuel gas and as such is invariant with respect to chemical reaction. Mixture fraction is transported by convection and diffusion through the flame and its stoichiometric contour defines the flame reaction zone.

The mixture fraction field is obtained by modelling the diffusion flames under investigation. Transport of momentum, mass and energy need to be considered to specify the flame. Fast chemistry assumptions for the major reactions are assumed and the radiation influenced temperature field is obtained from measurements. Soot formation rates in the flames are deduced from measured soot concentrations combined with the modelled velocity field.

Soot reaction rates are generally considered to be slow compared with the major reactions (Kent and Wagner, 1984, Kennedy 1988) at least over part of the flames. In these regions soot formation rates should in principle be determined from the local environment and an increase in flame residence time leads to increased soot concentrations. Alternatively, if soot reaction rates are fast, then soot formation is controlled by gas mixing rates as for the major species. Soot yields are then constant and not a function of residence time.

In previous work (Kent and Honnery, 1989), four flames with differing residence times were examined. The soot formation rates ( $\text{kg/m}^3\text{-s}$ ) and the soot yields ( $\text{kg/s soot/kg/s carbon in fuel}$ ) were compared at equivalent flame heights using fraction of fuel burned as the normalizing variable. It was found that the longer residence time flames have lower soot formation rates and that ultimately the maximum soot yields do not vary much with residence time. This implied that overall the soot yields are mixing controlled. However, the longer residence time flames also have lower temperatures because of greater radiation losses and this may be the reason for the lower formation rates rather than the slower mixing rates in the longer flames.

The objective of the present work is to examine the soot formation rates in two of these flames in terms of the measured local temperatures as well as mixture fractions. We wish to determine whether temperature is the missing parameter required to explain the differences in the soot formation rates between the flames as well as examining how well this two-variable correlation works for different flames.

### EXPERIMENT

The fuel is ethylene issuing from a 10.7mm diameter vertical nozzle into still air. Two concentric wire screens surround the length of the flame at diameters of 35mm and 70mm. The two flame conditions investigated are shown in Table 1. Residence times are computed along the the flame centrelines from the nozzle to the calculated stoichiometric length defined where the mixture fraction  $f=0.064$ .

Table 1: Flame conditions

Flame	Fuel flow Rate (ml/s)	Stoich. length (cm)	Residence Time (s)	Max. soot yld.
1	4.77	8.8	0.111	0.25
2	11.6	24.0	0.164	0.29

A detailed description of the experimental technique appears in Kent and Honnery (1989) and only a brief outline is given here. Soot volume fraction is measured by the extinction of a focused laser beam at 633nm (d'Alessio et al., 1973). Rayleigh absorption is assumed using  $1.94 - 0.54i$  for the soot refractive index (Lee and Tien, 1981). The path measurement data is collected by continuous automated data collection as the flame traverses the optics. These radial profiles are then converted to point measurements by Abel inversion at radial intervals of 0.1mm. Radial profiles are repeated at vertical intervals of 5mm for flame 1 and 10mm for flame 2.

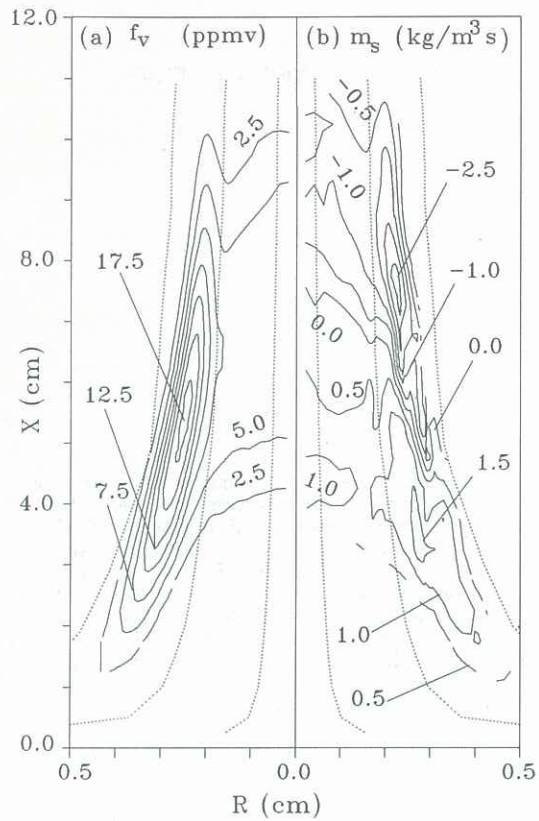


Figure 1. (a) Soot volume fraction for flame 1 and some typical particle trajectories. (b) Soot formation rates for flame 1.

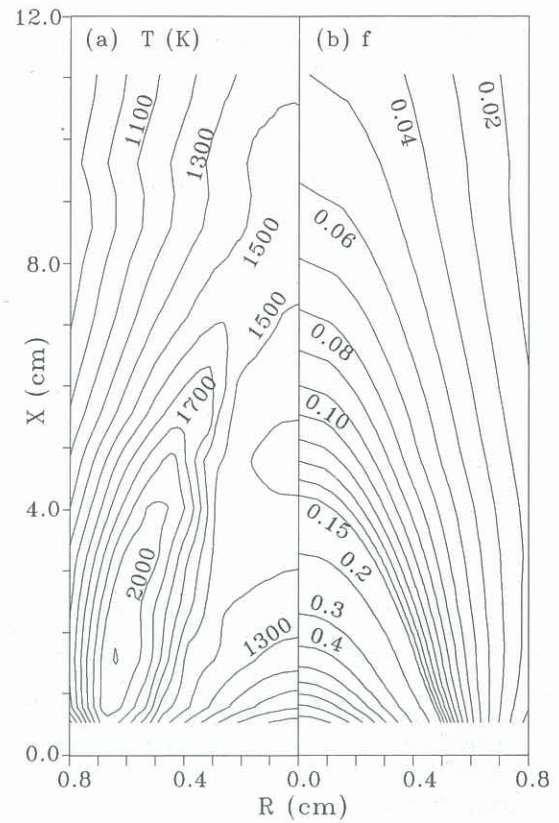


Figure 3. (a) Measured temperatures for flame 1. (b) Predicted mixture fraction for flame 1.

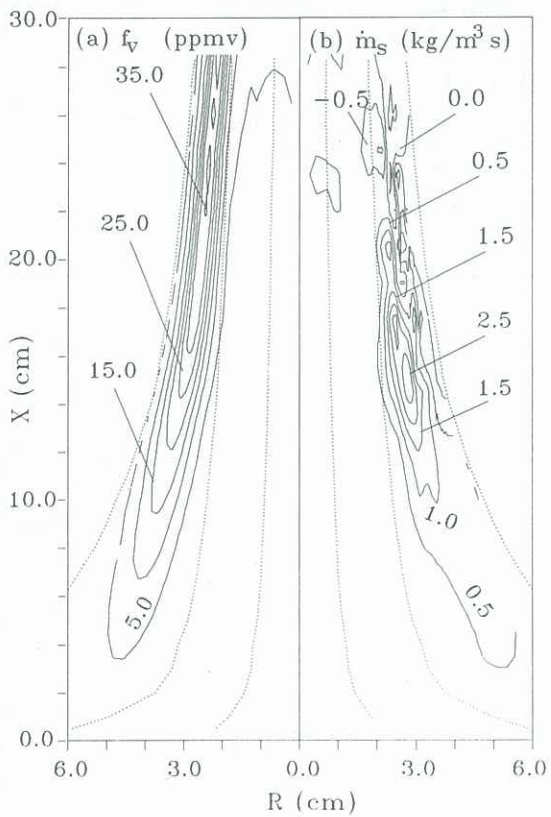


Figure 2. (a) Soot volume fraction for flame 2 and some typical particle trajectories. (b) Soot formation rates for flame 2.

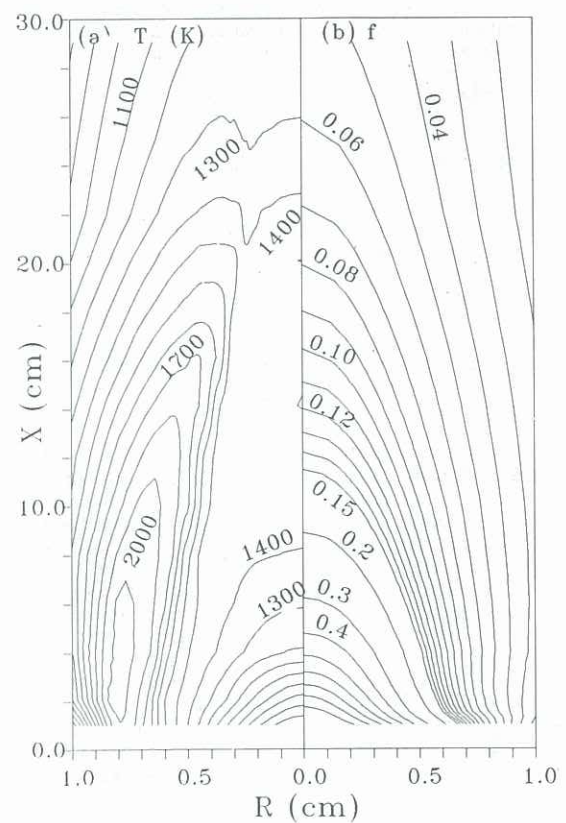


Figure 4. (a) Measured temperatures for flame 2. (b) Predicted mixture fraction for flame 2.

Figures 1a and 2a show the measured soot volume fractions,  $f_v$ , as contour maps for both flames. Flame 1 is the smaller flame in which the soot formed is completely burned out as evidenced by the decreasing volume fractions towards the end of the flame. Its peak volume fractions of 18ppmv occur in a thin annular region on the rich side of the reaction zone. Some soot is also found near the centreline although in lower concentrations of around 5ppmv. In flame 2, much of the soot produced escapes as smoke due to lower temperatures which freeze oxidation. This flame exhibits the same annular structure as flame 1 although the peak concentrations are higher, around 35ppmv, and they extend well past the stoichiometric length of 24cm.

Despite the difference in peak soot concentrations between the flames, the maximum soot yields (before the onset of burnout) computed from the modelled velocities fields are similar as shown in Table 1. That is flame 1 has a shorter residence time, but a higher average soot formation rate than flame 2.

Temperatures are measured using bare platinum rhodium thermocouples with bead diameters in the range 190–230 $\mu$ m. A rapid insertion technique (Kent and Honnery, 1989) is used to minimise the soot deposition effects. Radiation corrections are applied to the thermocouple reading using a bead emissivity of about 0.2. The correction amounted to about 160K at an indicated temperature of 1900k.

The temperature fields for the flames are shown in Figs. 3a and 4a. The characteristics are a temperature ridge near the stoichiometric contour, and decreasing temperatures with height due to radiation losses. The differences between the flames can be seen by comparing temperatures at equivalent mixture fractions. Beyond the stoichiometric length, flame 2 temperatures are some 100 – 150K lower than flame 1.

#### FLAME FIELD PREDICTIONS

Determination of the soot formation rate requires the velocity, density and mixture fraction fields throughout the flames. These quantities are obtained by modelling the flame field using well known methods (Bilger, 1976, Kent and Honnery, 1987). The approach is to relate the major species concentrations to the chemically conserved scalar, the mixture fraction, and to solve its transport equation to obtain species profiles. The assumptions are that major species reactions are fast compared with molecular diffusion rates, so diffusion rates control reaction rates, and that the diffusivities of all species are equal.

The transport equations of momentum and mixture fraction are solved for axisymmetric flow using a streamline coordinate transformation. The flow is parabolic and the boundary layer assumptions are made that the transverse pressure gradient and longitudinal diffusion fluxes are negligible. Buoyancy forces are included in the momentum equation. The mixture fraction has no source or sink term in its transport equation, has a value of unity at the fuel jet and is zero in the surrounding air. The predicted mixture fraction fields for both flames are shown in Figs. 3b and 4b. The main reaction zone is the  $f = 0.064$  contour.

Validation of the model has been carried out (Kent and Honnery, 1989) by comparison against non-sooting flame temperature measurements. Corrections to the theoretically derived transport coefficients of 10% are required to match the computed flame field to the measured reaction zone.

#### SOOT FORMATION RATES

The soot growth rates in the flame are determined along computed particle trajectories by numerically differentiating the measured soot concentrations and using the computed velocity field. The diffusion of soot particles is considered to be negligible. Thermophoretic

forces (Friedlander, 1977) on the soot particles from the steep radial temperature gradients are included and cause significant deviations in the particle trajectories.

Particles are traced from the first measurement plane just above the fuel nozzle. Since differentiation exaggerates scatter in measurements, the soot volume fraction profiles were smoothed slightly before processing. Sensitivity of the derived formation rates to the thermophoretic velocity component was checked by setting it to zero. Only small changes in the peak formation and burnout rates were found.

The derived soot formation rates for both flames are shown in Figs. 1b and 2b along with sample trajectories. Both flames exhibit strong growth just below their regions of peak soot concentrations. These regions are derived from trajectories that have passed through the flame reaction zone and become aligned with the mixture fraction contours.

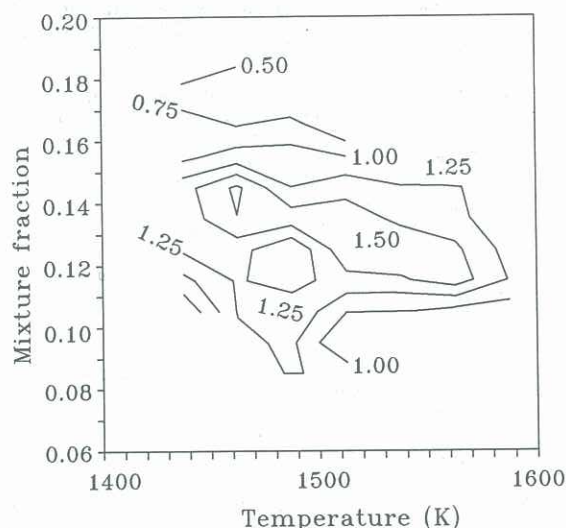


Figure 5. Soot formation rates ( $\text{kg}/\text{m}^3\text{-s}$ ) correlated against mixture fraction and temperature for flame 1.

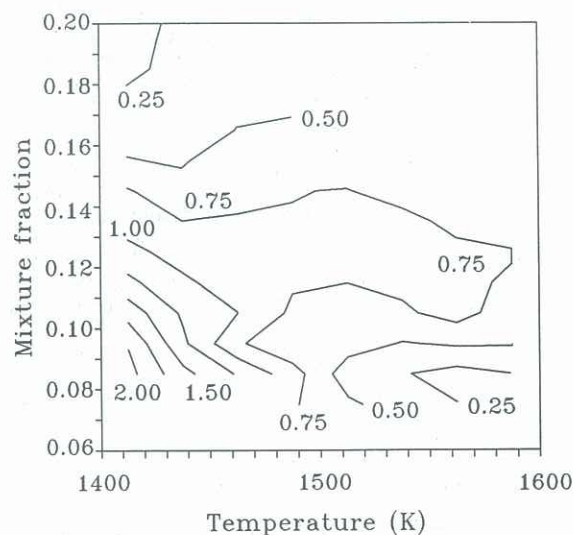


Figure 6. Soot formation rates ( $\text{kg}/\text{m}^3\text{-s}$ ) correlated against mixture fraction and temperature for flame 2.

The peak formation rates in flame 1 of about  $1.5\text{kg/m}^3\text{-s}$  are found in the mixture fraction range 0.12 to 0.15 and temperatures of 1450 to 1600K. Formation also extends towards the centreline in this flame. The peak formation rates in flame 2 are about  $2.5\text{kg/m}^3\text{-s}$  and are found in the mixture fraction range 0.09 to 0.11 and temperatures of 1400 – 1500K. Flame 2, however, does not exhibit the strong growth of flame 1 in the centreline region and its high growth region is relatively less extensive than for flame 1.

The soot formation rates are correlated with temperature and mixture fraction by allocating them to temperature intervals of 25K and mixture fraction intervals of 0.01. The resulting average soot formation rate maps for the two flames are shown in Figs. 5 and 6. Only data from regions of significant growth have been included in these maps to avoid scatter from low formation rate regions.

Both maps show that soot formation occurs in a relatively narrow temperature and mixture fraction band which both flames have in common. Flame 2 shows high formation rates in a small region of the map. However over a large part of the map, the soot formation rates for flame 1 are up to twice as high as for flame 2.

In the temperature range from 1450–1525K and mixture fraction 0.1 to 0.14 formation rates for flame 1 range from 1.25 to  $1.5\text{kg/m}^3\text{-s}$  and for flame 2 they are mostly 0.5 to  $0.75\text{kg/m}^3\text{-s}$ . There are typically 4 – 40 entries in an interval and the standard deviation is typically 5 – 15% of the average. A factor of two difference between the flames is therefore statistically significant.

## CONCLUSIONS

The soot formation correlation maps show that formation occurs in a band of mixture fraction and temperature for both flames, but the formation rate varies between the flames for given values of these parameters.

The previous work on these flames found that flame 1 had higher average formation rates than flame 2, as evidenced by the almost equal maximum soot yields for both flames, and temperature was considered as a possible cause. The correlation maps here indicate that it is not temperature which is causing the higher formation rates since these occur at the same temperatures. This conclusion depends on the reliability of the thermocouple temperature measurements in sooting regions of the flame. Errors in temperature measurements would tend to lower the indicated temperatures of flame 2 more than flame 1 because of higher soot concentrations. Therefore it is safe to say that even with temperature measurement errors, the lower formation rates in flame 2 are not occurring at lower temperatures than for flame 1.

The difference in formation rates between the flames can be caused by other factors. Soot surface area and particle age may be considerations. The smaller flame has younger particles which may be more reactive. However the influence of the gas diffusion rates in the flame, the rates at which reactants come together, is the first consideration. The larger flame has lower diffusion rates (Kent and Honnery, 1989) and if soot formation chemistry is faster than the mixing rates, then the diffusion rates will control the formation rates. The results here strengthen the case that mixing rates have an important influence over soot formation rates in these flames.

## ACKNOWLEDGEMENTS

This work is supported by the Australian Research Council and the Aeronautical Research Laboratories.

## REFERENCES

Bilger, R.W. (1976) Progress in Energy and Combustion Science. 1:87–109

D'Alessio A., Di Lorenzo, A., Beretta, F. and Venitozzi, C. (1973) Fourteenth Symposium (International) on Combustion, The Combustion Institute, Pittsburgh. pp.941–953

Friedlander, S.K. (1977) Smoke, Dust and Haze, Wiley.

Frenklach, M. and Warnatz, J. (1987) Combustion Science and Technology 51:265–283

Honnery, D.R. and Kent J.H. (1989) Submitted to Combustion and Flame.

Kennedy, I.M. (1988) Combustion, Science and Technology. 59:107–121

Kent, J.H. and Wagner, H.G. (1984) Combustion Science and Technology, 41:245–269.

Kent, J.H. and Honnery, D. (1987) Combustion Science and Technology 54:383–397

Kent, J.H. and Honnery, D.R. (1989) Combustion and Flame (in press)

Lee, S.C. and Tien, C.L. (1981) Eighteenth Symposium (International) on Combustion, The Combustion Institute, Pittsburgh. pp.1159–1166